

# Erosion of Polymer Pellets during Blending in a Twin-Screw Extruder

Hongbing Chen, Uttandaraman Sundararaj, and Krishnaswamy Nandakumar

Dept. of Chemical and Materials Engineering, University of Alberta, Edmonton, Alberta T6G 2G6, Canada

Mark D. Wetzel

E. I. du Pont de Nemours and Co., Inc., Experimental Station, Rte. 141 and Henry Clay, Wilmington, DE 19880

DOI 10.1002/aic.10701

Published online October 24, 2005 in Wiley InterScience (www.interscience.wiley.com).

Keywords: erosion, polymer breakup, polymer blend, on-line visualization, extrusion

## Introduction

The behavior of Newtonian droplet deformation and breakup has been well established through a fundamental study by Taylor<sup>1,2</sup> and other researchers (such as Grace<sup>3</sup> and Bentley and Leal<sup>4</sup>). It is well known that polymeric drops are usually highly non-Newtonian fluids. Their behavior under even a simple shear flow may not follow the prediction by theories for Newtonian fluids.<sup>5-9</sup> The mechanism of polymer drop deformation and breakup has been intensively studied to understand the development of morphology of polymer blends during blending, such as in twin-screw extruders (TSEs).<sup>10-14</sup>

On-line visualization provides the most direct way to study the polymer blending process and polymer drop deformation and breakup.<sup>13,15,16</sup> Lin et al.<sup>12</sup> reported an "erosion" mechanism for polycarbonate (PC) drop in a polyethylene (PE) matrix under simple shear flow with viscosity ratio  $> 4$ . In this report of our current study, the blending process of the same PE/PC blend in a TSE was visualized on-line to study the deformation and breakup of PC pellets in a PE matrix under complex flow. A sliding-barrel mechanism was used to perform the on-line visualization through a glass window fitted in the barrel.

## Experimental

A 40-mm corotating TSE was used for this study. The detailed description about the device used for the on-line visualization can be found in our previous report.<sup>17</sup> The extruder consisted of nine barrel sections, and the whole barrel was

mounted on two parallel slides. By moving the whole barrel along the screws, we can visualize the process at different sections through one glass window, and map the pressure and temperature profiles along the channel using several pressure and temperature probes mounted at different angular positions in one spacer plate fitted in the barrel. The extruder was configured with a standard melting zone screw and was operated in an open-discharge mode. A glass window was fitted in one of the nine barrels. A spacer plate was installed upstream of the barrel with the glass window. The distance between the spacer plate and the glass window was 90 mm. Figure 1 shows the sliding mechanism, screw configuration, and initial locations of the glass window and spacer plate. Pressure transducers and thermocouples were mounted in the spacer plate at several angular locations to obtain an averaged pressure and temperature at each slide position.

The slide started at the retracted position ( $X = 0$  mm). The operation was allowed to stabilize for at least 2 min at each position before recording the video and measuring pressure and temperature. After finishing measurements at one position, the barrel was moved to the next slide position to take the video and measure the pressure and temperature. The melting process was visualized through the glass window at each slide position using a digital camera or high-speed video recording device (2000 frames/s).

Two polymers were used in this study: PE (PetroMont DMDA-8920) was the matrix phase and PC (GE Lexan 140) was the dispersed phase. Properties of these two polymers are summarized by Lin et al.<sup>12</sup> PE pellets are initially white, opaque, and spherical in shape, and PC pellets are transparent and cylindrical in shape. The feed to the extruder consisted of 90 wt % PE and 10 wt % PC with a total mass flow rate at 22.7 kg/h. The screw speed was constant at 40 rpm. The tempera-

Correspondence concerning this article should be addressed to U. Sundararaj at u.sundararaj@ualberta.ca.

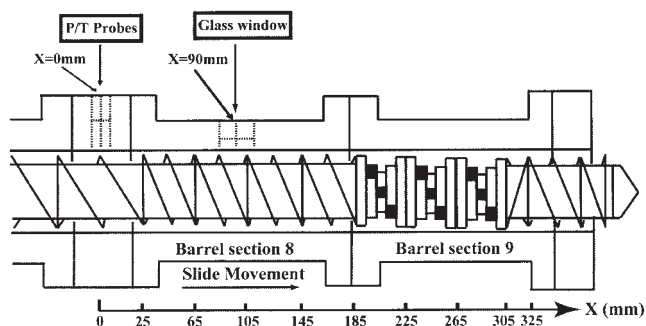


**Figure 1. Sliding-barrel mechanism, screw configuration, and initial position of P/T probes and glass window.**

The screw was made of conveying screw elements ( $X < 185$  mm), followed by three forward kneading blocks ( $X = 185$ – $305$  mm), a reverse pumping element ( $X = 305$  to  $325$  mm), and then the conveying pumping screws ( $X > 325$  mm).

tures for barrels 1 to 9 were set as ( $^{\circ}\text{C}$ ): 50, 50, 150, 150, 160, 220, 230, 250, and 250, respectively.

## Results and Discussion

This study focused on the kneading section and part of the conveying section in the TSE, where intensive melting and mixing occurred. Figure 2 shows the temperature and pressure profiles along the screw channel. Because the barrel could be moved, although the screws were fixed in the  $X$ -direction, each slide position  $X$  corresponds to a physical screw location:  $X = 0$  mm corresponds to the initial location of the spacer plate, which is located between barrel section 7 and barrel section 8, and is around 1200 mm from the initial feed location. There was an  $8^{\circ}\text{C}$  temperature increase from  $X = 0$  mm to  $X = 190$  mm, and a relatively constant temperature was achieved in the kneading section ( $\sim 220^{\circ}\text{C}$  from  $X = 190$  to  $X = 325$  mm). The pressure was built up monotonically from  $X = 150$  mm to  $X = 290$  mm (upstream of the reverse flow element,  $X = 305$  mm).

Figure 3 shows a series of still pictures taken with a digital

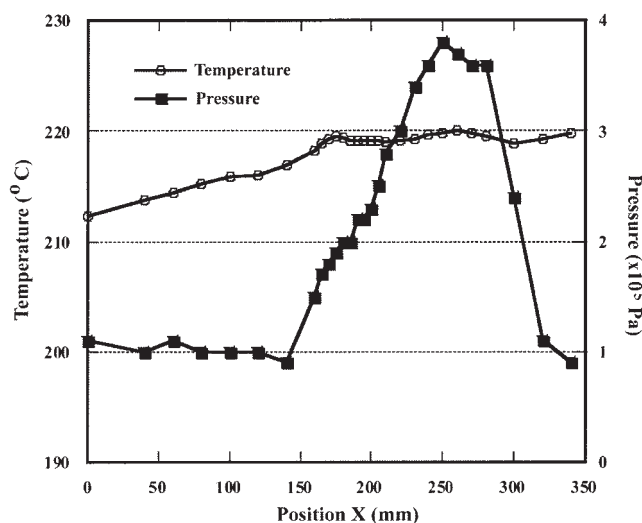


**Figure 2. Temperature and pressure profiles along the extrusion channel.**

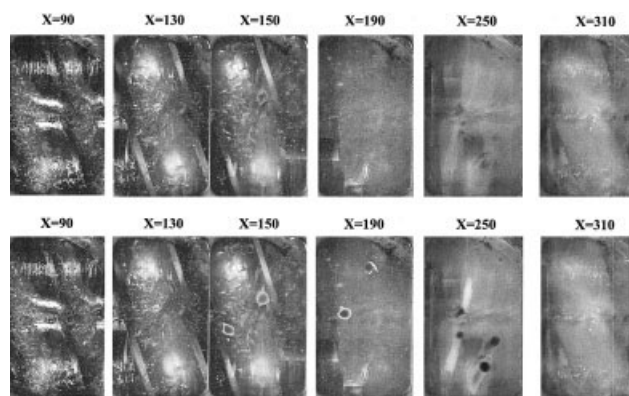


**Figure 3. On-line visualization of the PE/PC blending process in the TSE.**

Top row: original pictures; bottom row: "erosion" of some PC pellets is schematically highlighted in corresponding images (value for  $X$  in mm).

camera at different slide positions. The dimension of the glass window is 40 mm in length and 30 mm in width ( $X$ -direction). Still pictures were taken at every 20 mm in the  $X$ -direction. The barrel temperature for most sections was set appreciably above the PE melting temperature,  $T_m$  ( $\sim 145^{\circ}\text{C}$ ). PE melted in the conveying section mainly as a result of heat conduction from the hot barrel. When the flow reached the screw location  $X = 90$  mm, the majority of PE in the blend had already melted. The melted PE was transparent (see Figure 3). The black screw root can be seen from pictures at  $X = 90$  mm. Most PC pellets in these regions were still transparent, in solid state, and kept their original shape. From our previous article, pressure profile and visualization results were used to determine the location of the transition region of melting process in the TSE.<sup>17</sup> The transition region in a TSE usually occurred at the screw location just before the pressure started to build up and the solid concentration in the flow was high. For the PE/PC system studied here, most PE had already melted at  $X = 130$  mm, a dilute PE melt suspension with PC pellets had formed at  $X = 130$  mm (see Figure 3), and the pressure had started to build up at  $X = 150$  mm (see Figure 2). The PE/PC blending process under the current operating conditions has a very short transition region (limited to the region around  $X = 130$  mm). The channel was fully filled with PE melt suspension at  $X = 150$  mm. The monotonic increase in pressure after  $X = 150$  mm also indicated that the channel was completely filled with a dilute polymer melt suspension.

As the flow approached  $X = 150$  mm, the mixture changed to a more milky appearance. Most PC pellets in the picture at  $X = 150$  mm still retained their original cylindrical shape. However, whitening of some PC pellets on their surfaces is shown at  $X = 150$  mm. PC pellets that are surrounded with a cloud of PC melt can be identified. The softened outer layer of PC pellets was stretched and peeled off from the pellets in the flow. The "erosion" mechanism is shown for some PC pellets, which means the outer layer of PC pellets softened, stretched, and peeled off from the pellets under the complex flow (Figure 3 at  $X = 150$  mm). This erosion mechanism continued to dominate the deformation and breakup of PC pellets in the kneading section of the TSE (see Figure 3 from  $X = 190$  to  $X = 250$  mm). Stretched ribbons are found for many PC pellets in

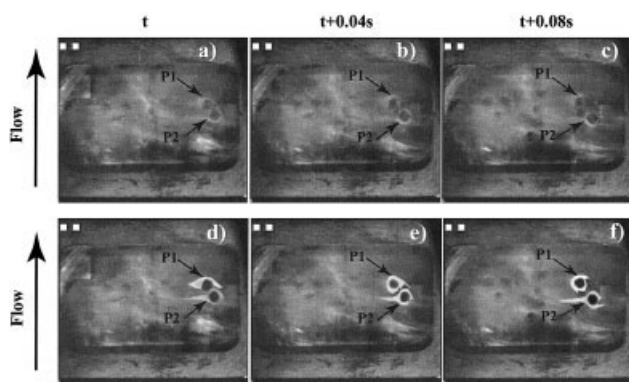


**Figure 4. High-speed video images at  $X = 210$  mm; two PC pellets are marked as P1 and P2.**

Top row: original images: (a) time  $t$ ; (b) time  $t + 0.04$  s; (c) time  $t + 0.08$  s. Bottom row: corresponding images where erosion of two PC pellets, P1 and P2, is schematically highlighted: (d) time  $t$ ; (e) time  $t + 0.04$  s; (f) time  $t + 0.08$  s. Similar behavior is found for other PC pellets.

the PE flow. Through this erosion mechanism, the size of PC pellets was reduced and the shape of PC pellets was changed from cylindrical to spherical. As more PC dispersed into the PE matrix under complex flow in the kneading section, the flow became more milky, and a more uniform flow was reached at  $X = 310$  mm.

In these experiments, the temperature measured is not the real melt temperature but rather the temperature of the inner surface of the barrel. However, the temperature profile still gave a good approximation of the real temperature of the melt in the channel.<sup>17</sup> The flow temperature in the kneading section was relatively constant at 220°C, which is around 30°C lower than the PC processing temperature. However, this temperature matches the temperature set up in a model experiment for PC drop deformation and breakup in a PE melt under simple shear flow.<sup>12</sup> The same erosion mechanism was found for PC drops in the PE melt under simple shear flow and complex flow in the TSE. The viscosity ratio of PC with PE at this temperature was  $>4$ , especially when considering the possible temperature gradient in PC pellets. No breakup occurs in Newtonian systems with viscosity ratio  $> 4$  in shear flow,<sup>1</sup> although this result is not always true for polymer systems. Breakup of PC drops was found in the PE melt under both simple shear flow<sup>12</sup> and complex flow in a TSE (this study). For a dilute polymer melt suspension, friction between dispersed particles no longer plays an important role for the deformation and breakup of PC pellets. Viscoelastic properties and viscosity gradient in PC pellets could explain this erosion mechanism under the conditions studied here. It should be noted that this work used one system at one set of operating conditions for the TSE. It is believed that the erosion mechanism occurs in other systems processed in a TSE, although this still needs to be investigated.

Figure 4 shows images from a high-speed video at  $X = 210$  mm (Figures 4a–4c), and what was observed in the high-speed video for some PC pellets is schematically highlighted (Figures 4d–4f). The time interval between each image was 0.04 s. From the continuous images, we can track the movement and breakup mechanism of PC pellets in the flow. Two PC pellets are marked as P1 and P2 in Figure 4a, and their locations were tracked in the following images to study their movement. P1

and P2 were very close to each other initially (Figures 4a and 4d) and 0.08 s later, P1 moved downstream and P2 moved upstream (Figures 4c and 4f). At the same time, both pellets also rotated along the  $X$ -direction. For the screw configuration studied here, the back flow in the kneading section occurred mainly in the intermeshing region. Self-rotation along the axis perpendicular to the  $X$ -direction can be found in the high-speed video for some PC pellets in the intermeshing region. Erosion of PC pellets in the PE melt is clearly shown in these high-speed video images (see especially the highlighted PC pellets). This erosion mechanism was also found for a polystyrene/polypropylene (PS/PP) blend in a TSE.<sup>17</sup> Both the PS/PP blend and the PE/PC blend represent a wide range of polymer blends in terms of melting behavior during processing. Therefore, erosion is thought to be one of the dominant mechanisms for polymer pellet deformation and breakup in melt processing.

## Conclusions

The deformation and breakup of PC pellets in a PE melt under complex flow in a TSE were visualized on-line using a sliding-barrel mechanism. High barrel temperatures were set for the conveying section so that a dilute PE melt suspension with PC pellets was formed in the kneading section. High-speed video was recorded to track the movement and breakup mechanism of PC pellets in a PE flow. Erosion was found to be the dominant mechanism for the PC pellets breaking up in the PE matrix under complex flow in the TSE. Self-rotation of PC pellets along the axis in both the  $X$ -direction and its perpendicular direction was shown in the high-speed video results. The on-line visualization result shows that erosion could be a major mechanism for the deformation and breakup of polymer pellets in extrusion.

## Literature Cited

1. Taylor GI. The viscosity of a fluid containing small drops of another fluid. *Proc R Soc Lond A Phys Sci.* 1932;138:41–48.
2. Taylor GI. The formation of emulsions in definable fields of flow. *Proc R Soc Lond A Phys Sci.* 1934;146:501–523.
3. Grace HP. Dispersion phenomena in high viscosity immiscible fluid systems and applications of static mixers as dispersion devices in such systems. *Chem Eng Commun.* 1982;14:225–277.
4. Bentley BJ, Leal LG. An experimental investigation of drop deformation and breakup in steady, two-dimensional linear flows. *J Fluid Mech.* 1986;167:241–283.
5. Wu S. Formation of dispersed phase in incompatible polymer blends: Interfacial and rheological effects. *Polym Eng Sci.* 1987;27:335–343.
6. Sundararaj U, Macosko CW. Drop breakup and coalescence in polymer blends: The effects of concentration and compatibilization. *Macromolecules.* 1995;28:2647–2657.
7. Sundararaj U, Dori Y, Macosko CW. Sheet formation in immiscible polymer blends: Model experiments on initial blend morphology. *Polymer.* 1995;36:1957–1968.
8. Levitt L, Macosko CW, Pearson SD. Influence of normal stress difference on polymer drop deformation. *Polym Eng Sci.* 1996;36:1647–1655.
9. Migler KB. String formation in sheared polymer blends: Coalescence, breakup, and finite size effects. *Phys Rev Lett.* 2001;86:1023–1026.
10. Sundararaj U, Macosko CW, Rolando RJ, Chan HT. Morphology development in polymer blends. *Polym Eng Sci.* 1992;32:1814–1823.
11. Migler KB. Droplet vorticity alignment in model polymer blend. *J Rheol.* 2000;44:277–290.
12. Lin B, Sundararaj U, Mighri F, Huneault MA. Erosion and breakup of polymer drops under simple shear in high viscosity ratio system. *Polym Eng Sci.* 2003;43:891–904.
13. Lin B, Mighri F, Huneault MA, Sundararaj U. Parallel breakup of

- polymer drops under simple shear. *Macromol Rapid Commun.* 2003; 24:783-788.
14. Chen H, Sundararaj U, Nandakumar K. Modeling of polymer melting, drop deformation and breakup under shear flow. *Polym Eng Sci.* 2004;44:1258-1266.
  15. Sakai T. The development of online techniques and novel processing systems for the monitoring and handling of the evolution of microstructure in nonreactive and reactive polymer systems. *Adv Polym Technol.* 1995;14:277-290.
  16. Wetzel MD. Experimental study of LDPE melting in a twin-screw extruder using on-line visualization and axial pressure and temperature measurements. *SPE ANTEC Tech Papers.* 2002.
  17. Chen H, Sundararaj U, Nandakumar K, Wetzel MD. Investigation of the melting mechanism in a twin-screw extruder using a pulse method and online measurement. *Ind Eng Chem Res.* 2004;43:6822-6831.

*Manuscript received Jun. 3, 2005, and revision received Aug. 26, 2005.*